NUCL SCI TECH (2019) 30:177
https://doi.org/10.1007/s41365-019-0697-9

Phase-stabilized RF transmission system based on LLRF controller and optical delay line

Jia-Ji Liu[1,2] · Xin-Peng Ma[1,2] · Guo-Xi Pei[1,2] · Nan Gan[1,2] · Ji-Sen Yang[1,2]

Received: 4 June 2019 / Revised: 30 September 2019 / Accepted: 1 October 2019 / Published online: 15 November 2019
© China Science Publishing & Media Ltd. (Science Press), Shanghai Institute of Applied Physics, the Chinese Academy of Sciences, Chinese Nuclear Society and Springer Nature Singapore Pte Ltd. 2019

Abstract Radio frequency (RF) transmission systems with high-precision phase stability are required by the next generation of particle colliders and light sources. An RF transmission system was designed to meet this requirement. In this system, RF signal generated at the sending end is modulated onto a continuous wave (CW) optical carrier, transmitted through an optical fiber, and demodulated at the receiving end. The phase drift is detected by a digital phase monitor with femtosecond-level accuracy and compensated by a motorized optical fiber delay line (ODL). The measurement results show that the long-term phase drifts can be stabilized to within 100 fs (pk–pk), 500 fs (pk–pk), and 1.8 ps (pk–pk) in a 400-meter-long optical fiber over 1 h, 24 h, and 10 days, respectively.

Keywords RF transmission · Phase-stable optical fiber · Phase drift · Phase noise · Femtosecond · Picosecond · Digital phase monitor

1 Introduction

An important factor that influences the operation stability of particle colliders and light sources driven by accelerators is the phase synchronization accuracy within the entire facility. The next generation of particle colliders requires RF phase synchronization between each node with sub-picosecond-level accuracy. Light sources, which have higher-precision requirements, require femtosecond-level accuracy. An RF transmission system is used to assign the standard RF phase to each node of the accelerator. RF phase errors introduced in the transmission route will lead to phase inconsistency of the nodes and affect the performance of the entire accelerator. To meet the needs of system synchronization, the stability of the RF transmission system is also a critical requirement.

There are numerous approaches for transmitting RF reference signals, among which coaxial cable-based systems and optical fiber-based systems are the most common solutions. Coaxial cable-based systems are robust and reliable but only suitable for short-range or low-accuracy RF transmission systems. The European XFEL used both cable and optical links in its RF distribution system with phase drifts of the coaxial and optical links in the sub-1 ps and sub-10 fs ranges, respectively [1]. Optical fiber-based systems mainly employ two technologies, the CW-based system and the pulse-based system. The CW-based system was conceived at the Atacama Large Millimeter Array (ALMA) [2] and first applied in accelerators by Lawrence Berkeley National Laboratory (LBNL) [3]. LBNL used interferometrically stabilized optical fibers and the optical heterodyning technique in its optical transmission system and demonstrated phase jitter and drift of less than 20 fs (rms) in 2.2 km of optical fiber over 60 h [4]. The SPring-8

This work was supported by the Foundation of the Key Laboratory of Particle Acceleration Physics and Technology of Chinese Academy of Sciences (No. 29201531231141001)

✉ Xin-Peng Ma
maxp@ihep.ac.cn

[1] Institute of High Energy Physics, Chinese Academy of Sciences, Beijing 100049, China

[2] University of Chinese Academy of Sciences, Beijing 100049, China

Angstrom Compact Free Electron Laser (SACLA) used similar techniques in its double-loop optical fiber length stabilization system. The phase drift for a 400-meter-long optical fiber was suppressed to within 50 fs (pk–pk) [5]. The Libera Sync 3 CW reference clock transfer system from Instrumentation Technologies achieves phase stability of tens of femtoseconds by using an electronic phase detector [6]. The pulse-based system was first proposed by the Massachusetts Institute of Technology (MIT). The Deutsches Elektronen Synchrotron (DESY) has also performed research on similar techniques. The pulse-based system can achieve sub-fs synchronization accuracy and is mainly used on XFEL to synchronize timing between laser and laser, or laser and RF signal [7, 8].

The High Energy Photon Source (HEPS) currently under construction and the planned Circular Electron Positron Collider (CEPC) of the Institute of High Energy Physics (IHEP) both have urgent needs for RF transmission systems. CEPC will be the biggest circular electron positron collider in the world with a circumference of 100 km. The requirement of the phase synchronization accuracy for CEPC is 0.2° (RMS) within 24 h, corresponding to about 200 fs (RMS) at 2856 MHz [9]. HEPS has similar requirements.

To meet these requirements, an RF transmission system with high-accuracy phase stabilization was developed. The RF reference signal is modulated onto a CW optical carrier, transmitted via a single-mode optical fiber and demodulated at the receiving end. Due to the temperature characteristics of the fiber, ambient temperature variations will lead to optical path changes and cause phase drift in the RF signal. A feedback loop was designed to eliminate the phase drift. By directly demodulating the reflected optical signal and comparing it with the local RF signal, the complexity of the optical heterodyning technique is avoided. A digital phase monitor based on ADC and FPGA is adopted instead of the traditional electronic phase detector, and ODL, which has a wider adjustment range than piezoelectric fiber stretcher, is used to compensate the phase drift. As the optical fiber is a key component of the RF transmission system, a phase-stable optical fiber cable from Yangtze Company (YPSOC) with good temperature performance is used as the transmission medium.

As the RF transmission system is a component of a large facility, reliability and low maintenance are critical requirements. The operation principle of our system is simple and reliable, and the components are technologically mature and readily available commercial products. The system is applicable in actual facilities.

2 System concept description

The layout of the phase drift compensation mechanism is shown in Fig. 1. The phase drift $\Delta\phi$ of the entire system is mainly introduced by the long optical fiber. The optical wave is reflected by FRM at the receiving end back into the same optical fiber, which introduces another phase drift of $\Delta\phi$. The phase change observed at the reflecting end is twice that observed at the receiving end. The phase difference between the local and the reflected RF signals carries information of the phase change in the long optical fiber. A proportional (P) control algorithm is used to stabilize the phase at the very end of the link by maintaining a constant level of the phase difference between the local and reflected RF signals. Only slow phase drifts, which are within the bandwidth of the feedback loop, will be suppressed.

Temperature changes will also cause phase drifts in the devices and optic fiber patch cords at the sending and receiving ends. Symmetrical phase errors inside the feedback loop, right from the optical circulator, can be removed. The phase errors in parts of these modules located outside of the feedback loop can be reduced by controlling the temperature of the sending and receiving ends.

The layout of the RF transmission system is shown in Fig. 2. The system is divided into three modules: the RF transmission module, the RF phase monitor module, and the software module.

In the RF transmission module, a 2856 MHz RF signal is generated by a Keysight Analog Signal Generator (ASG), modulated onto 1550 nm CW laser generated by an RIO Narrow Linewidth Laser through an electro-optical modulator (E/O) and transmitted to the receiving end. The optical wave will be reflected back along the same fiber by the FRM at the receiving end. Two discovery semiconductors photoelectric detectors (O/Es) are used to restore the RF signal. As optical devices such as E/O and optical connectors cause optical power loss, an erbium-doped optical fiber amplifier (EDFA) is added.

The RF phase monitor module is composed of the RF front-end chassis and MicroTCA chassis. The RF front-end chassis converts the 2856 MHz RF signal down to a

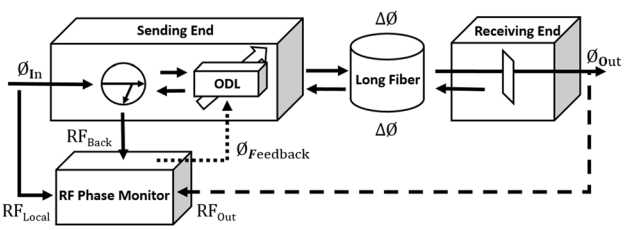

Fig. 1 Layout of the phase drift compensation mechanism

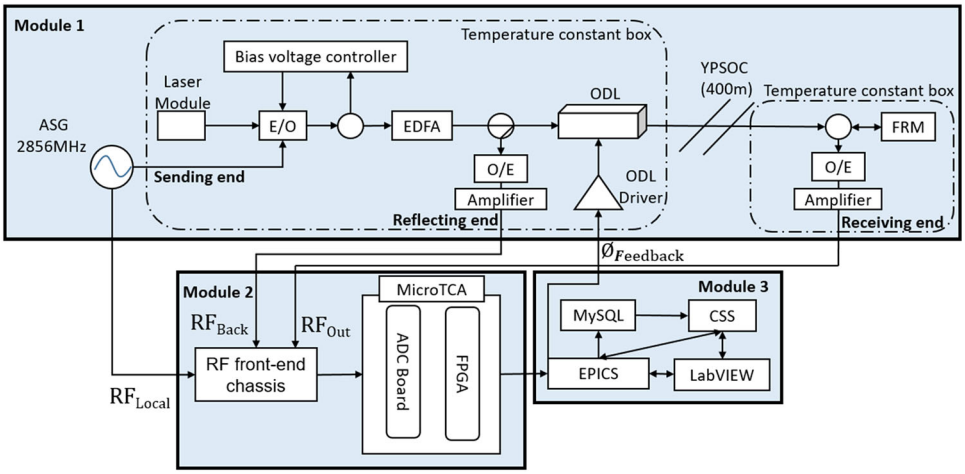

Fig. 2 Layout of the RF transmission system

23.8 MHz intermediate frequency (IF) signal. The IF signal is sampled by a 16-bit ADC with a sampling rate of 95.2 MSPS and processed on a MicroTCA-based FPGA board to calculate the signal phase. The phase information is then transmitted to the software module.

The software module is used for acquiring and processing the phase information, passing the feedback parameters to ODL, and designing the interaction interface.

3 System components design and test

3.1 Phase-stable optical fiber

In a long-range RF transmission system, many factors like mechanical vibration and humidity and temperature changes will cause length variation of the optical fiber, which will result in phase drift of the RF signal loaded on the laser. The thermal coefficient of delay (TCD) is a key parameter of an optical fiber and quantifies the resistance of the optical fiber to temperature change. TCD can be quantified by the following formula:

$$\mathrm{TCD} = \frac{\Delta t}{\Delta T \times \Delta L}, \tag{1}$$

Δt is time delay, ΔT is temperature change, ΔL is light length change in the optical fiber. The TCDs of most standard single-mode fibers (such as Corning SMF-28e) are between 33.4 and 42.7 ps/km/K [10]. This means that for 1000-meter-long optical fibers, the time delay is from 33.4 to 42.7 ps when the temperature changes by 1 °C.

There are some phase-stable optical fiber products with low TCD. For example, the TCDs of phase-stable optical fiber (PSOF) from Furukawa and Strong Tether Fiber Optic Cable (STFOC) from Linden Photonics are below 5 ps/km/K and 7 ps/km/K, respectively [10, 11]. Using such optical fibers instead of traditional ones can reduce the phase drift caused by temperature change. YPSOC is a newly developed phase-stable optical fiber that can replace PSOF and STFOC.

A TCD measurement experiment was designed and carried out to determine the temperature performance of YPSOC. A 400-meter-long YPSOC was placed inside a temperature control box. The ambient temperature of YPSOC was controlled by setting the interior temperature of the temperature control box. A temperature probe was pasted onto the fiber and attached to a temperature detector. A time delay detector system (similar to the RF transmission system in this article) was used to detect the time delay.

Figure 3 shows the delay and TCD of YPSOC vs. temperature change. As the temperature changes from 17.2 to 45.6 °C, the time delay is 83 ps. According to Eq. 1, the average TCD of YPSOC is 7.3 ps/km/K when the temperature is between 17.2 and 45.6 °C. As TCD varies with temperature, the TCD is calculated in different temperature intervals of 5 °C. The results are plotted as the red line in Fig. 3. The TCD increases from 5 ps/km/K to 10.5 ps/km/K as the temperature increases from 17.2 to 45.6 °C. In general, the TCD of YPSOC is about 7 ps/km/K at the normal temperature (about 25–35 °C) of the accelerator gallery.

Mechanical fiber length adjustment devices have limited adjustable ranges. The phase drift will fall outside the adjustable range for long transmission distances and large

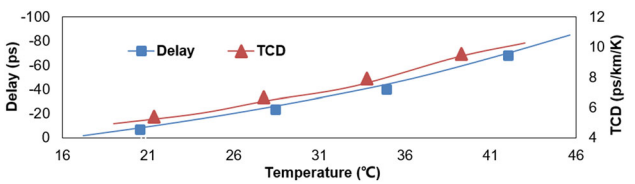

Fig. 3 (Color online) Delay and TCD of YPSOC versus temperature changes

temperature variations. The use of phase-stable optical fibers is a good solution to this problem. Therefore, YPSOC can be used in future ultra-long-range or ultra-high-accuracy RF transmission systems due to its good temperature performance.

3.2 Temperature control box

To test the temperature performance of YPSOC, a temperature control box was designed. The box is made of aluminum, which has good thermal conductivity, and covered by thermal insulation material to isolate heat changes. The key components of the temperature control box are a temperature probe, a temperature controller, and a Peltier cooling unit. The temperature probe is attached to the inner wall of the aluminum box to monitor the temperature inside the box and transmit the temperature to the temperature controller. The temperature controller controls the cooling or heating effect of the Peltier cooling unit by providing current to it. A wind-cooled radiator is used to cool the Peltier unit when the unit is working in refrigeration mode. The layout of the temperature control box is shown in Fig. 4.

Another function of the temperature control box is to maintain the interior temperatures of both the sending and receiving ends. Components like the laser module, the EDFA and the RF signal amplifier generate heat when operating. There are numerous optical elements and fiber patch cords that will introduce phase drift due to the temperature change in the sending and receiving ends. The performance of electronic devices can also be affected by temperature change. Therefore, temperature control is needed at both the sending and receiving ends.

Figure 5 shows the performance of the temperature control box at the sending end where the laser module and the EDFA are the main heat sources which make the temperature difficult to control. The temperature change of the temperature control box was maintained to within $\pm$ 0.01 °C over 48 h while the room temperature changed by 1.5 °C.

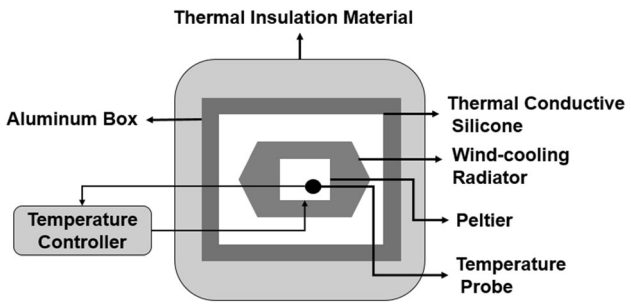

Fig. 4 Layout of the temperature control box

3.3 RF phase monitor module and software module

In the RF phase monitor module, an improved digital signal processing frame is used for the accelerator low-level RF control system. ADC and FPGA boards are adopted to sample and calculate the RF phase [12]. Figure 6 shows the basic framework of the RF phase monitor module.

Using a GHz-level ADC cannot meet the requirement of low-noise measurement and will increase the difficulty of the FPGA calculation, because of the introduction of phase noise. Therefore, the RF signal is converted down to a 23.8 MHz (f_i) IF signal by an RF front-end module. The IF signal is sampled by a 16-bit ADC with a sampling rate of 95.2 MSPS (f_s) and processed on a MicroTCA-based FPGA board. The digital signal sampled by the ADC is mixed in the FPGA through a multiplier. The in-phase/quadrature (I / Q) is then demodulated according to the ratio of the IF frequency and the sampling rate (f_i/f_s).

If the ratio satisfies Eq. 2, the digital IF signals are exactly orthogonal to each other in phase. Using I and Q to represent two adjacent sampled signals, the data flow can be represented as $...I, Q, -I, -Q$ .... Equation 3 indicates that subtracting the signals every other clock cycle can eliminate the direct current noise introduced by the ADC circuit, I' and Q' are signals after being processed.

$$\frac{f_i}{f_s} = \frac{2m-1}{4} (m = 2n-1, n \in N) \tag{2}$$

$$I' = \frac{I_n - (-I_{n-1})}{2}, Q' = \frac{Q_n - (-Q_{n-1})}{2} \quad (n \in N) \tag{3}$$

To further suppress the noise introduced by the ADC, I/Q digital signals are average filtered by a cascaded integrator–comb (CIC) filter with 5 MHz bandwidth [13]. Using a Coordinate Rotation Digital Computer, the phases ϕ are calculated via Eq. 4 [14, 15]. The results are then transmitted to the Experimental Physics and Industrial Control System (EPICS).

$$\phi = \arctan \frac{I'}{Q'} \tag{4}$$

As shown in Fig. 7, the core of the software module is EPICS. EPICS receives the phase information from the FPGA and processes data with the assistance of LabVIEW. EPICS communicates with LabVIEW through the Data-logging and Supervisory Control (DSC) module.

The differential phase scheme is used to calculate the phase error. The reference (local) RF signal and the measured (reflected) RF signal are monitored simultaneously, and the phase difference between them is taken for feedback control. This method can eliminate the local noise from ASG and the common mode phase error caused by the ADC.

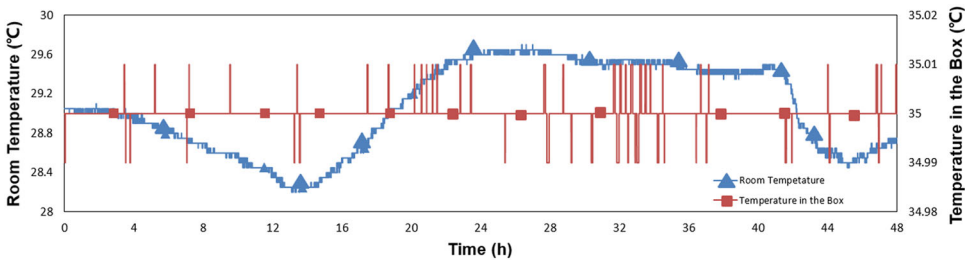

Fig. 5 (Color online) Temperature stability measurement results of the temperature control box

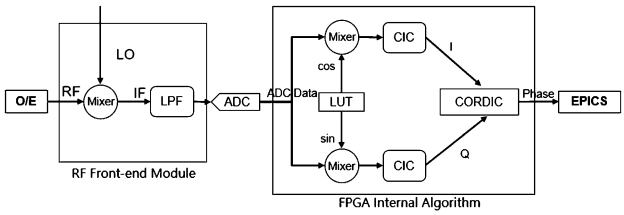

Fig. 6 Basic framework of the RF phase monitor module

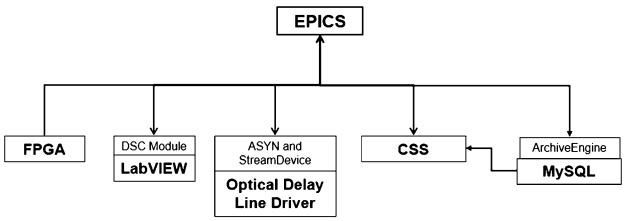

Fig. 7 Software module architecture

EPICS communicates with the ODL through a RS-232 serial port by the Asyn and Streamdevice modules. The interaction interface used to monitor phase drifts and ODL working condition and control the switching on or off of the feedback system is designed by Control System Studio (CSS).

A database was established to store and query experimental data such as the phase information during operation. The Relational Database Channel Archiver collects data from the input/output controllers and writes the data into a relational database. This system can implement and test the archiver with MySQL database. Users can access historic and live data from the database using CSS Data Browser.

3.4 RF phase noise measurement

RF phase noises at both the receiving and reflecting ends are important considerations for the stability of the RF transmission system. Phase noises were measured by a phase noise analyzer from ROHDE & SCHWARZ. No filter was added.

Phase noise is present in the RF signal generated by ASG. Active devices like the E/O, O/E, and amplifier will also introduce phase noise. A 2856 MHz/5 dBm RF signal is generated as the sample. As shown in Fig. 8, the phase

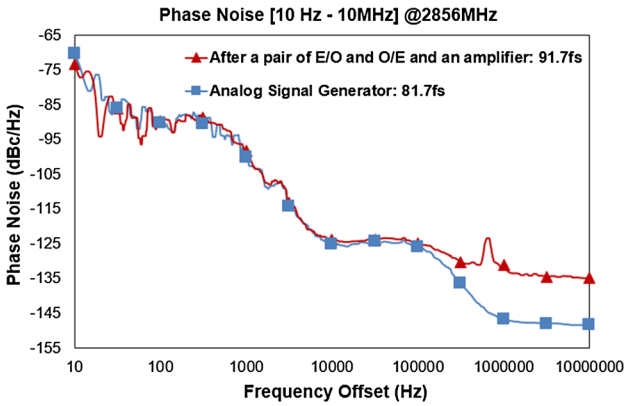

Fig. 8 (Color online) Phase noises of the RF signal generated by ASG and after a set of E/O, O/E and amplifier

noise from ASG was 81.7 fs (RMS) (10 Hz–10 MHz). After the RF signal has passed through a set of E/O, O/E, and amplifier, the phase noise increased by 10 fs.

The optical fiber is also a noise source. Nonlinear effects (like stimulated scattering, self-phase modulation, cross-phase modulation, and four-wave mixing) and linear impairments (like chromatic dispersion, polarization mode dispersion, polarization-dependent loss, and Rayleigh scattering) in the optical fiber will degrade the transmission characteristics and decrease the signal-to-noise ratio [16, 17].

In this system, a single-mode fiber is used for bidirectional information transmission using the same light source, optical fiber, and beam coupler. Such a transmission mode can reduce the connection complexity and system cost and improve the system performance [18]. However, there is a drawback to bidirectional transmission: The backscattered Rayleigh light of the optical fiber will increase the system noise [19]. In this optical loop, the forward signal wavelength is reused as the reflected signal wavelength by FRM, so the reflected signal wavelength is the same as the forward one. The transmission performance will be reduced by the interference noise arising from Rayleigh backscattering (RB) [20].

Figure 9 shows two upstream paths of the RB signal. In one case, the backscattered forward signal influences the reflected signal. In the other case, the reflected signal by FRM is backscattered and re-reflected by RFM and

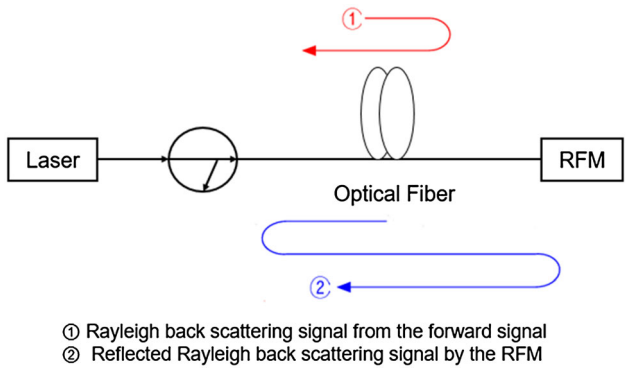

Fig. 9 Two paths of RB signals in upstream

influences the reflected signal. The former case occurs in both the forward and reflected signals, but the latter case only occurs in the reflected signal [21]. In addition, as the power of the forward wave is higher than that of the reflected wave, RB noise will increase with the light power. Thus, the RB upstream noise is increased.

To test the influence of fibers with different lengths on the RF phase noise, 100-m, 500-m, and 1000-m SMF-28e fibers were selected as the transmission mediums for bidirectional information transmission. The RF phase noises at both the receiving and reflecting ends were measured. The results are shown in Fig. 10. The phase noises at the receiving end are under 100 fs (RMS) (within 1000 m), while the phase noise at the reflecting end is larger than that at the receiving end for a given fiber. The phase noise reaches 164.4 fs (RMS) at the reflecting end when the fiber length is 1000 m. This is almost twice as large as the phase noise at the receiving end.

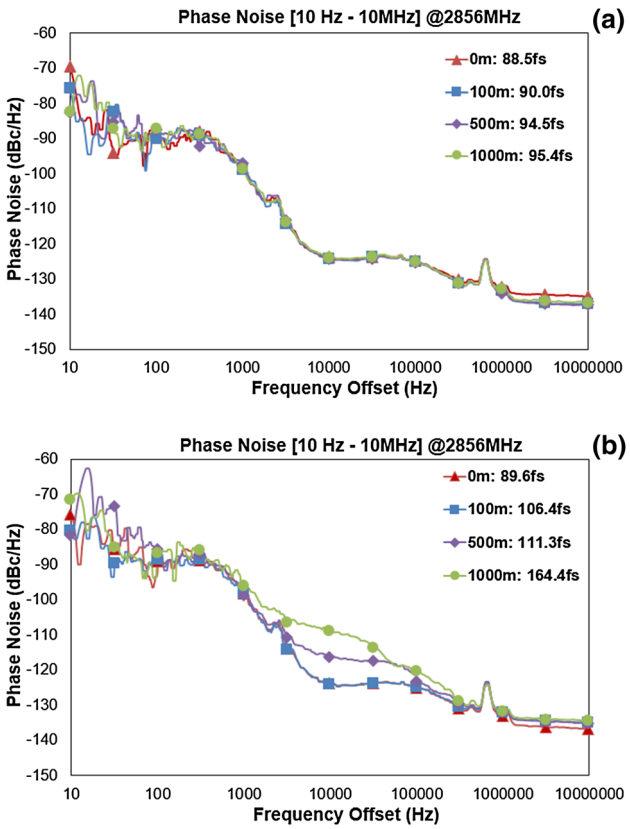

Fig. 10 (Color online) Phase noises at the receiving end (**a**) and the reflecting end (**b**) with different lengths of fibers

The phase noise increases with the transmission distance, especially at the reflecting end. If the transmission distance is increased to dozens of kilometers, RB will be much more prominent, and the phase noise will be a major issue for the phase stability of the RF transmission system. The main methods to reduce RB are spectral broadening, polarization control, and frequency shifting [22].

4 System performance measurement results

After designing and manufacturing the whole system, some tests were carried out to evaluate the system performance. As shown in Fig. 2, 400-m-long YPSOC was used as the transmission line without temperature control. The output RF phase was measured by the RF phase monitor and compared with the local RF phase.

The phase drift of the open-loop system in this configuration was measured over 12 h. As shown in Fig. 11, the phase drifts of the received signal and the reflected signal were 3 ps (pk–pk) and 6 ps (pk–pk), respectively, while the room temperature changed by 0.6 °C. The results are in accordance with the phase drift compensation principle.

The phase drifts of the closed-loop system were then measured over 1 h, 24 h, and 10 d. In Fig. 12, the in-loop (within the bandwidth of the feedback loop) phase drift is the phase difference between the reflected and local RF signals. The out-of-loop (out of the bandwidth of the feedback loop) phase drift is the phase difference between the received and local RF signals.

The in-loop phase drifts were suppressed to within 100 fs (pk–pk) at all times. It can be seen from each lower graph that the variation trends of the phase compensated by ODL are consistent with the temperature change. That means that the ODL has worked properly and compensated for the phase drifts due to the temperature change. As

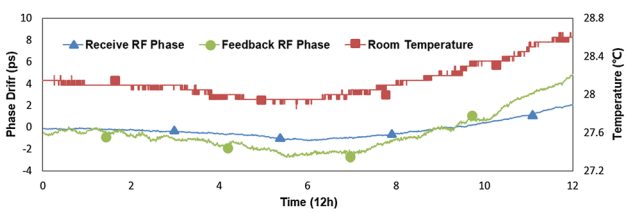

Fig. 11 (Color online) Open-loop RF phase drifts at both the receiving and reflecting ends over 12 h

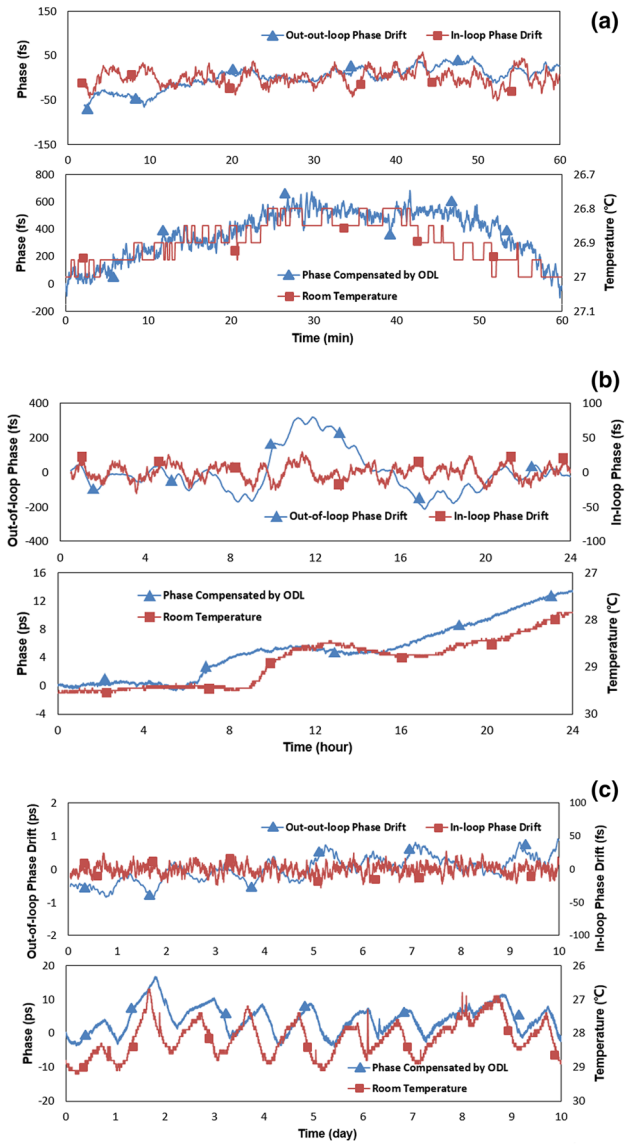

Fig. 12 (Color online) Experimental system results with closed-loop. In-loop and out-of-loop phase drifts, ambient temperature changes and ODL running conditions over 1 h, 24 h, and 10 days are shown in **a**–**c**. All phase drift data have been normalized and moving averaged (intervals: **a** 2 min, **b** 20 min, and **c** 1 h)

shown in Fig. 12a, 600-fs phase error was compensated by ODL when the temperature changed by 0.2 °C, and the out-of-loop phase drift was suppressed to 100 fs (pk–pk) over 1 h. In Fig. 12b, 13-ps phase error was compensated by ODL when the temperature changed by 1.5 °C, and the out-of-loop phase drift was 500 fs (pk–pk) for 24 h. Figure 12c shows the result for a long-term system run. As the temperature changed by 2 °C over 10 days, the out-of-loop phase drift was maintained to within 1.8 ps (pk–pk). The presented results show that our system can fulfill the design requirements.

In addition to the limit of the feedback bandwidth, the remaining phase error reflected in the out-of-loop phase drift may be caused by the absence of temperature control in the RF front-end module and humidity control in the whole system. The large phase noise of the reflected RF signal, which lowers the precision of the phase detection, may also contribute to the phase error. These problems will be investigated and resolved in the next experiment.

5 Conclusion and outlooks

An RF transmission system has been designed and manufactured. The digital signal processing frame used in the RF phase monitor was designed according to the low-level RF control system, and it achieved femtosecond-level phase detection accuracy. LabVIEW was integrated into the software architecture to process data flexibly. A phase-stable optical fiber with good measured temperature performance of 7 ps/km/K was used in the experiment. It was found that RB has a great influence on the phase noise of the reflected signal and that phase noise increases with the fiber length. It has been experimentally demonstrated that the long-term out-of-loop phase drifts in the transmission of 2856 MHz RF signal through a 400-meter-long cable could be suppressed to within 100 fs (pk–pk) and 500 fs (pk–pk) over 1 h and 24 h, respectively. The stability requirement (200 fs (RMS) for 24 h) of the RF transmission system can be fulfilled. There is still room for system optimization.

For the next experiment, improved components like low-noise signal sources and faster phase shifters will be incorporated to minimize the system noise and enlarge the feedback-loop bandwidth. An integration (I) and differentiation (D) control algorithm will be added to eliminate the residual produced by the P control algorithm. Studies on the optical heterodyning technique and RB noise are also planned. High-precision RF transmission systems should work in demanding environments. Any possible error sources like ambient temperature change and air shock have to be considered to obtain high accuracy in such a complex and large system. Stricter environment control will be implemented in the next experiment. Further, another receiving end module will be incorporated so that uncorrelated (point-to-point) drift can be further evaluated by detecting the phase drift of the two independent receiving channels.

References

1. P. Jatczak, D. Kolcz, F. Ludwig et al., RF phase reference distribution for the European XFEL, in *Low Level Radio Frequency Workshop, Shanghai, China*, Nov, 2017, pp. 03–06
2. B. Shillue, A. Sarmad, L. D. Addario, The ALMA 1st local oscillator reference. http://library.nrao.edu/public/memos/alma/memo483.pdf/
3. J.W. Staples, R. Wilcox, FROA004: Fiber transmission stabilization by optical heterodyning techniques and synchronization of mode-locked laser using two spectral lines, in *International Free Electron Laser Conference, Palo Alto, CA, USA*, 21–26 Aug 2005
4. R. Wilcox, J.M. Byrd, L. Doolittle et al., Stable transmission of radio frequency signals on fiber links using interferometric delay sensing. Opt. Lett. **20**, 3050–3052 (2009). https://doi.org/10.1364/OL.34.003050
5. M. Hirokazu, O. Takashi, O. Yuji, et al., WEOBB01: Design and performance of the optical fiber length stabilization system for SACLA, in *nternational Particle Accelerator Conference, Dresden, Germany*, 16–20 Jun 2014. https://doi.org/10.18429/JACoW-IPAC2014-WEOBB01
6. P. Orel, E. Janezic, P. Lemut, et al., TUPRI079: Test results of the Libera Sync 3 CW reference clock transfer system, in *International Particle Accelerator Conference, Dresden, Germany*, 16–20 June 2014. https://doi.org/10.18429/JACoW-IPAC2014-TUPRI079
7. M.Y. Peng, Sub-femtosecond optical timing distribution for next-generation light sources. Ph.D. Thesis, Massachusetts Institute of Technology (2015)
8. C. Sydlo, M. Czwalinna,M. Felber, et al., WEP047: Femtosecond timing distribution at the European XFEL, in *International Free Electron Laser Conference, Daejeon, Korea*, 23–28 Aug 2015. https://doi.org/10.18429/JACoW-FEL2015-WEP047
9. The CEPC Study Group. CEPC conceptual design report, volume I—Accelerator. https://arxiv.org/ftp/arxiv/papers/1809/
10. M. Bousonville, K.M. Bock, M. Felber, et al., MOPG033: New phase stable optical fiber, in *Beam Instrumentation Workshop, Virginia, USA*, 15–19 Apr 2012
11. Kashyap. US patent 4923278, Inventor, Temperature desensitization of delay in optical fibres, (1990)
12. R. Wilcox, J.M. Byrd, L. Doolittle, et al., JThA38: Phase stable RF-over-fiber transmission using heterodyne interferometry, in *National Fiber Optic Engineers Conference, San Diego, Canada*, 21–25 Mar 2010. https://doi.org/10.1364/NFOEC.2010.JThA38
13. M.P. Donadio, CIC filter introduction. http://www.dspguru.com/files/cic.pdf
14. J.E. Volder, The CORDIC trigonometric computing technique. IRE Trans. Electron. Comput. **3**, 330–334 (1959). https://doi.org/10.1109/TEC.1959.5222693
15. G. Huang, L.R. Doolittle, J.W. Staples et al., TUPSM082: Signal processing for high precision phase measurements, in *Beam Instrumentation Workshop, SantaFe, New Mexico, US*, 2–6 May (2010)
16. G.P. Agrawal, P.L. Kelley et al., *Nonlinear Fiber Optics*, 3rd edn. (Academic Press, Pittsburgh, 2001)
17. S. Jablonski, H. Schlarb, C.Sydlo, MOPB034: CW laser based phase reference distribution for particle accelerators, in *International Beam Instrumentation Conference, Melbourne, Australia*, 13–17 Sep 2015. https://doi.org/10.18429/JACoW-IBIC2015-MOPB034
18. O. Hitoshi, Bidirectional WDM transmission technique utilizing two identical sets of wavelengths for both directions over a single fiber. J. Lightwave Technol. **25**(1), 297–304 (2007). https://doi.org/10.1109/JLT.2006.887180
19. R.K. Staubli, P. Gysel, Statistical properties of single-mode fiber Rayleigh backscattered intensity and resulting detector current. IEEE Trans. Commun. **40**(6), 1091–1097 (1992). https://doi.org/10.1109/26.142799
20. J.M. Kang, S.K. Han, A novel hybrid WDM/SCM-PON sharing wavelength for up and down-Link using reflective semiconductor optical amplifier. IEEE Photonics Technol. Lett. **18**, 502–503 (2006). https://doi.org/10.1109/LPT.2005.863632
21. J.-M.Lee, D.-W. Lee, Y.-Y. Won, et al., JThA98: Reduction of Rayleigh Back-Scattering noise using RF tone, in *National Fiber Optic Engineers Conference, San Diego, CA, USA*, 24–28 Feb 2008. https://doi.org/10.1109/OFC.2008.4528133
22. T.H. Wood, N.J., Highlands. US patent 4879763, Optical fiber bidirectional transmission system (1989)